Nanoscience and Nanoengineering 2(1): 10-16, 2014
DOI: 10.13189/nn.2014.020102 http://www.hrpub.org

Bone-like Material, Synthesis, Optimization and Characterization

A. Elfalaky*, H.Hashem, T. Mohamed

Department of Physics, Faculty of Science, Zagazig University, Zagazig 44519, Egypt
*Corresponding Author: a.elfalaky@gmail.com

Abstract Nanocomposite hydroxyl apatite phase of calcium phosphate powder has been successfully synthesized employing coprecipitation technique. Structural characterization utilizing X-Ray Diffraction, SEM and FTIR techniques was achieved. To confirm the thermal stability of the obtained powder TGA and DSC measurements over wide range of temperatures were carried out. Moreover the dielectric constants ε' and ε'' were measured over wide range of temperature and frequency of applied electric field. Besides, density estimation was achieved by means of CT (ROI) for the obtained powder and compared with that of natural human bone. Finally the effect of Gamma-Ray on the density of nano calcium phosphate was investigated as a simulation to human bone.

Keywords Calcium Phosphate; hydroxyapatite; SEM; DSC; TG; Dielectric constants and CT

1. Introduction

Bone matrix mainly consists of calcium phosphate (CP). The phase of the CP constructing bone is hydroxyapatite (HAp). Bone is also a natural nanocomposite biomaterial with a complex structure. Bone-like materials are desired and essential for bone repair, bone cement and bone filler. Therefore bone regeneration research is demanded to deal with various clinical bone disease [1].

For Bone-like materials to be bioactive, bones and such materials must be compatible. In other words both must have similar physical properties. Regarding such bioactivity and compatibility; healing ability increases, possibility of foreign rejection decreases and formation of chemical bonds with surrounding hard tissues after implantation increases [2]. A chemical similarity between CP in HAp phase and bone has been recognized [3]. Accordingly, CP and HAp have been widely studied for bone regeneration and replacement, bone filling, bone engineering and drug delivery applications [4-5]. In order to attain bone-like material with physical properties resemble natural bone, it is necessary to measure physical properties of bone-likematerials and compare with that of the natural bone. For instance bone is a nanocomposite material, and then the bone-like material for better biocompatibility should be in nano form. It has also been confirmed that the application of external electric field enhances the bone healing [6]. Such enhancement was attributed to the fact that bone growth on bone-like material depends mainly on the permanent surface charge [7].

CP with HAp phase is one of most bone-like materials that similar to the inorganic part of human bone [8-9]. About 70% of the mass of living bone has chemical constitution of HAp. In addition HAp implant usually shows very good biocompatibility and good osteointegration [10]. It also forms chemical bonding with the surrounding hard tissues [2]. In this study it is aimed to fabricate CP in HAp phase with nano crystallite size. In addition, report some characterizations about structural analysis, dielectric constants, thermal stability and density. To compare the obtained data with those available corresponding to the human natural bone

2. Materials and Methods

CP of the chemical formula $Ca_5(PO_4)_3(OH)$ has been synthesized employing coprecipitation technique. In such a technique, aqueous solutions of high purity metal chlorides were mixed with $CO(NH_2)_2$. A chemical exchange reaction takes place according to the following:

$$5CaCl_2 + 3Na_2HPO_4 + CO(NH_2)_2 \longrightarrow$$

$$Ca_5(PO_4)_3(OH) + H_2O + 5NaCl + NaCN$$

Hydroxyapatite was recognized when the ratio between $CaCl_2$: Na_2HPO_4 was taken as 1.5:0.5 respectively. In addition the pH of the reaction medium was ~7.9. The reaction temperature was detected and found to be 100 ^oC. Filtering cycles were repeated many times until the pH reduces to 7 and no traces of NaCl were detected.

X-ray investigation has been performed utilizing Philips diffractometer (PW3040) with $CuK_{\alpha 1}$ with wave length λ = 1.5406 Å. Scanning electron microscope JeolJSM-6510LA was operated at 20 KV. The microstructure analysis was

performed using Scherrer method, Winfit and XPowder programs. Fourier-transform infraredspectroscopy (FT-IR) trace was recorded using Nicolet iS10 FT-IR Spectrometer. Pellets from powders of CP and KBr with ratio 1:50 were prepared for the IR examination. Disk shaped samples were prepared hydraulically under constant pressure (4 ton/cm^2). The dielectric constants of the disk shaped samples were measured over the temperature range of (293-573 K) with applied frequency from 50 Hz up to 5MHz using RCLBridge model Hioki 3532 Hitester. Differential Scanning Calorimetry (DSC) and Thermo-gravimetric Analysis (TGA) were carried out utilizing (Shimadzu DSC-50). Density estimation of nanocomposite CP in comparison with human bone was achieved using Computed Tomography (CT) (Siemens somatom definition 64). The effect of Gamma-Ray exposure on density of nanocomposite CP was investigated.

3. Results and Discussions

3.1. Structural and Analysis

Regarding the X-ray diffraction pattern Fig.(1) andJCPD 90-0432 card table (1), CP crystallizes in HAp phase with crystal structure of hexagonal system. The lattice constants of the hexagonal were calculated. Refinement of the unit cell and lattice parameters using XPowder program, yielded a =b = 9.3881 c = 6.8388 A$^\circ$ and unit cell volume = 521.99 $^\circ$A^3. The significant feature of the x-ray pattern, shown in Fig. (1), is the broadening of the reflection peaks. Such broadening indicates that the crystallites of the powder are of fine size. The crystallite size of the prepared powder was estimated utilizing three different techniques: Scherrer, Winfit and XPowder programs.

Scherrer relationship of the form [11]:

$$D = \frac{0.89\lambda}{\beta \cos\theta}$$

has been applied where D is the crystallite diameter, λ = 1.5406 Å, the wave length of the X-ray beam, β is the full width at half maximum of the reflected peak and θ is the Bragg's angle. The calculations indicate that the value of D is about ~ 6 nm. Utilizing Winfit program [12] the crystallite size was evaluated for the most intense peak at 2θ = 32.12º where the average value of D is ~ 5.85 nm. Also the crystallite size was estimated using the XPowder program [13] where the crystallite size was also estimated and found to be about 6 nm.

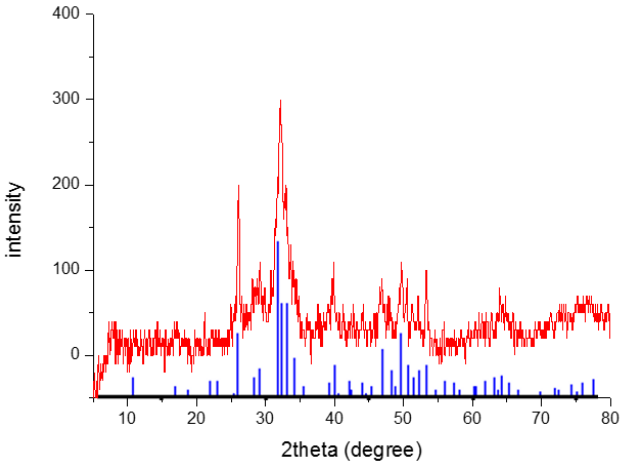

Figure 1. X-ray diffraction pattern for as prepared nano Calcium Phosphate.

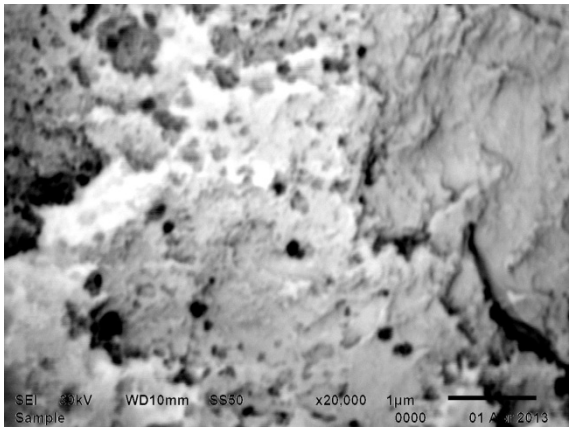

Figure 2. SEM of nano Calcium phosphates.

Scanning electron microscopy image is shown in Fig. (2). The micrograph reveals that different morphologies with some sort of aggregation, homogeneous distribution of the synthesized particle, and confirmed the presence of nanoparticles.

Table 1. X-ray data

Experimental data				JCPD 90-0432			
d(A°)	2θ	Intensity%		d(A°)	2θ	Intensity%	h k l
3.41593	26.065	66.6		3.44	25.879	40	0 0 2
3.05735	29.186	34.2		3.08	28.966	18	2 1 0
2.78137	32.157	100		2.814	31.773	100	2 1 1
2.69984	33.155	65.2		2.72	32.902	60	3 0 0
2.25620	39.926	38		2.262	39.818	20	3 1 0
1.93751	46.853	30.7		1.943	46.711	30	2 2 2
1.83185	49.733	37.3		1.841	49.468	40	2 1 3
1.71774	53.287	35.4		1.722	53.143	20	0 0 4
1.45412	63.975	22.4		1.452	64.078	13	3 04
a=b= 9.432 A°, c=6.881 A°, α = β = 90º and γ = 120º.							

3.2. FTIR

FTIR spectrum of the prepared CPis shown in Fig.(3). The broad transmittance band between 3700 and 3100 cm^{-1} has been assigned to the O-H stretch vibration of hydrogen bonded OH groups. It also revealed the presence of $CO_3^{-2}$with weak bands at (1456–1411 and 872 cm^{-1}). The bands at wave number 1033 and 960 cm^{-1} are assigned to the fundamental frequencies of the PO_4^{-3}groups (CaP groups). The bands at 603 and 562 cm^{-1} are assigned to the PO_4^{-4} groups [16-17]. Fig.(3) indicates that the prepared CP is of high purity.

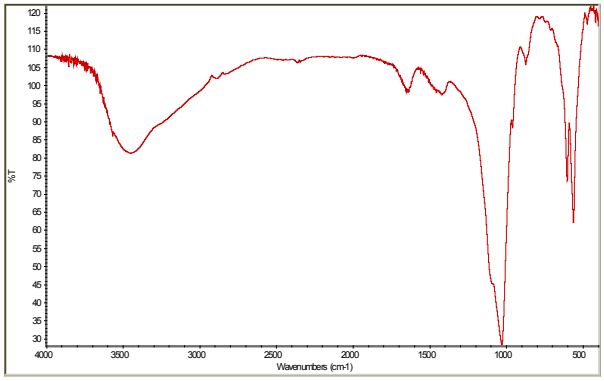

Figure 3. FT-IR for nano Calcium Phosphate.

The Force constant represents the strength of the bond and the restoring force per unit length of the bond elongation. The Force constant K was calculated using the following equation:-

$$\upsilon = \frac{1}{2\pi c}\sqrt{\frac{K}{\mu}}$$

where υ is the vibrational frequency of the bond, μ is the reduced mass of the bond and c is velocity of light. The calculated force constant of the assigned bands are shown in table (2). It can be seen that the force constant of the assigned groups is in order of 10^5dyn /cm. The most strong bond is the CaP group while the PO_4 group is the weakest one.

Table 2. The calculated force constant of the bond of all groups

Bond	absorption peak (cm^{-1})	force constant (dyne cm^{-1})x 10^5
O-H	3700	7.647
O-H	3100	5.368
CO_3^{-2}	1456	8.568
CO_3^{-2}	1411	8.047
CO_3^{-2}	872	3.073
PO_4^{-3}	1033	6.632
PO_4^{-3}	960	5.727
PO_4^{-4}	603	2.259
PO_4^{-4}	562	1.963

3.3. Dielectric Properties

Measurements of the dielectric constants, dielectric constant (ε') and dielectric loss (ε"), were carried out over wide range of temperature and frequency. Fig. (4) and Fig. (5) display the frequency dependence of both ε' and ε" at different temperatures respectively.

Dispersion occurs in the dielectric constant at the low frequency region (less than 22 KHz) where ε' decreases sharply with increasing frequency. For further increase in frequency the dielectric constant seems likely to be frequency independent. Such frequency dependence can be

attributed to polarization effect of the applied field where the increase in frequency tends to reduce the polarization due to the fast inversion of the applied field. Similar behavior has been reported for natural bone [16]. The dielectric constant of the nano CP at T=295K and frequency f=60 KHz is about 8.89 and that of the natural bone is 10. The effect of temperature in the dispersion region is significant than that in the high frequency region. Such trend can be attributed the interfacial polarization [17]. The dielectric loss ε" tends to decrease with the increase of the applied frequency as shown in Fig. (5). Dispersion was clearly observed in the frequency dependence. The inversely proportionality of the dielectric loss ε" with the applied field frequency is in agreement with that reported before [18].

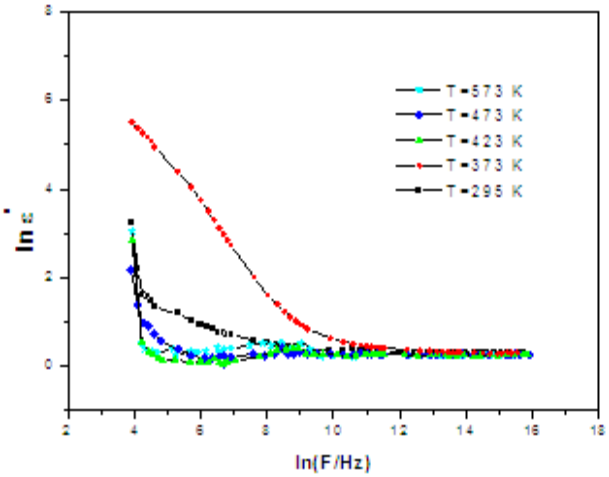

Figure 4. Frequency dependence of dielectric constant (ε') at different temperatures for Calcium Phosphate.

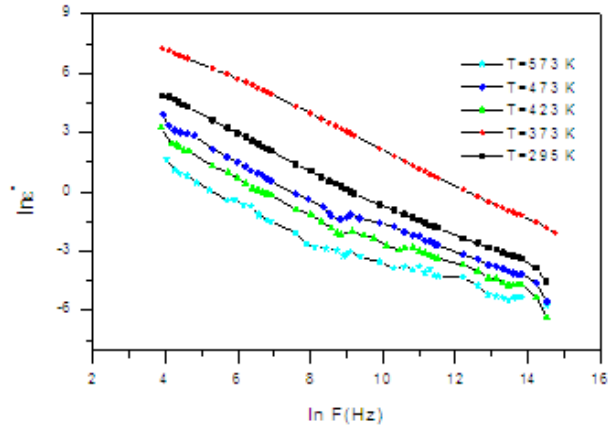

Figure 5. Frequency dependence of dielectric loss (ε") at different temperatures for Calcium Phosphate.

3.4. Thermal Properties

Fig. (6)represents the DSC measurements for nano CP in the range from 30-400 °C with rate 10 °C/min. The only detected transformation is characterized by a peak at temperature of 71 °C. Such results indicate that nano CP is hydrated, and this endothermic peak is duo to dehydration. It also indicates that there was no phase transformation taking place upon heating.

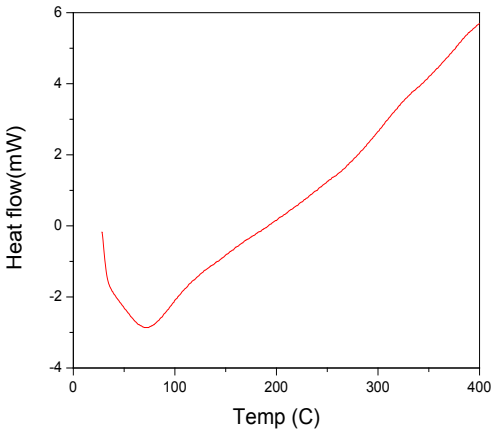

Figure 6. DSC of nanocomposite Calcium Phosphate

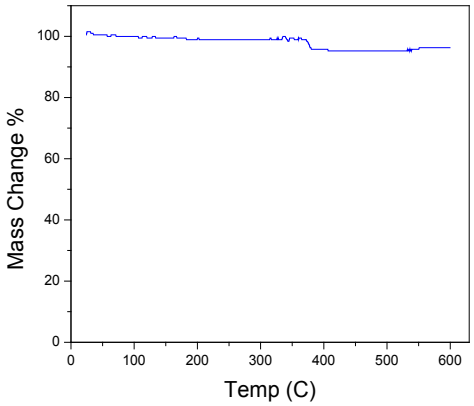

Figure 7. TGA of nanocomposite Calcium Phosphate

Mass loss against constant increase of temperature (TGA) is shown in Fig. (7). As shown, the mass loss of CP was around 5%. This result indicates that the prepared powder has excellent thermal stability even at high temperature. Furthermore, the small change of mass could be attributed to the partial removal of physically absorbed water and possibly lattice water [19].

3.5. Gamma-Ray (Radiation Exposure)

Radiation can be expressed in two aspects. The one that expresses the concentration of radiation at some point, or to a specific tissue and that express the total radiation delivered to a body. CP nanocomposite was exposed to Gamma-Ray by using Cobalt-60 (Co-60) as source, the dose was 15 gray (Gy). Computed tomography (CT) measuring Region of Interest (ROI) can be used as an indication of density, using X-ray attenuation. Figure (8) shows the ROI of nano CP and natural bone before exposing. For disk shaped nano CP, shown in Fig. (8-a), the value of ROI is 1057 HU. Values of ROI at different species of human bones are recorded in Fig. (8-b,c and d). The values of ROI are 636 - 1009 HU for pelvis bone, 1104-1438HU for skull bone, where HU is

Hounsfield unit. Such values are consistent with the previously reported value [20]. It worthy noted that the value of ROI depends on the pressure under which the disk sample is prepared. Consequently the pressure applied to the nano CP powder can be adjusted to have ROI comparable with that of the corresponding bone species.

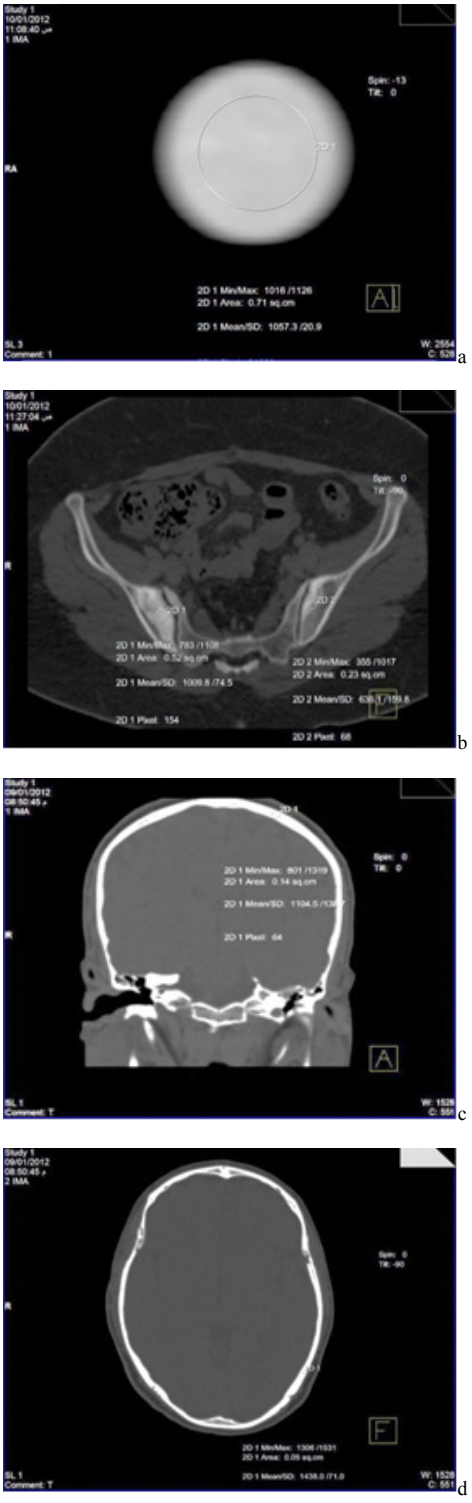

Figure 8. a, The ROI of Nano Calcium Phosphate before exposure. b, c, d The ROI of natural bone by CT

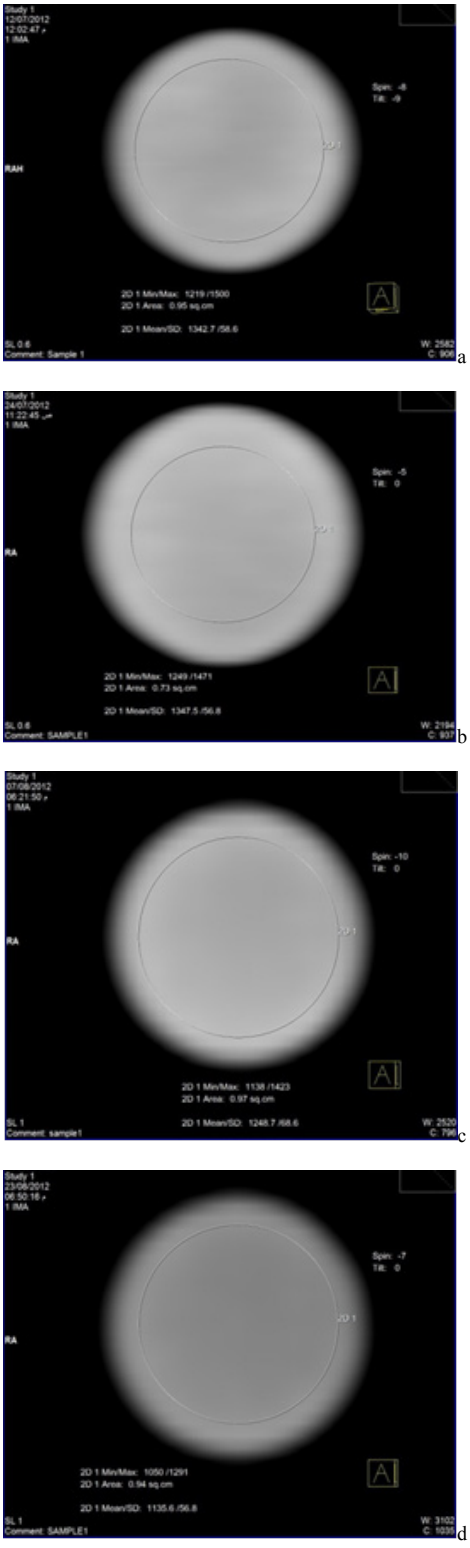

Figure 9. The ROI of Nano Calcium Phosphate after exposure, a 1 week, b 3 weeks, c 5 weeks, d 7 weeks

Bone mineral density BMD can be calculated using the formula [21]:

$$BMD = (HU + 95.51) / 868.0 \quad gcm^{-3}$$

where HU is Hounsfield unit (HU) which is given by [20]:

$$HU = (u_x - u_w) / (u_w - u_a)$$

where u_w and u_a are the linear attenuation coefficients of water and air, respectively. Thus, a change of one Hounsfield unit (HU) represents a change of 0.1% of the attenuation coefficient of water since the attenuation coefficient of air is nearly zero. CT scanners are calibrated with reference to water [20].

The disk shaped samples of nano CP were exposed to γ-rays for constant exposure time and then annealed at room temperature for certain time. Figure (9) illustrates nano CP after γ-rays exposure. Table 3 represents the ROI and BMD of nanocomposite CP after different annealing time. It has been found that the both ROI and BMD increase first with time. However after 5 week the ROI and BMD tend to decrease. Since the nanocomposite CP is stable then such variation can be attributed to the effect of γ-rays. It is known that γ-rays have significant effect on bonds in solids. The bond strength has been reported to be influenced by γ-rays [22]. In case of nanocomposite CP it can be said that γ-rays destroy the weakest bond associated with PO_4. The atoms of the broken bonds move to occupy the interstitial states in the crystal structure. Hence the density increases first. After 5 weeks of annealing at room temperature the bonds start toregenerate and the corresponding density decrease.

Table 3. TheROI and BMD of Calcium Phosphate before and after Exposure

Time after Exposure	ROI (HU)	BMD(g cm^{-3})
before	1057	1.32778
After 1 week	1342	1.65612
After 3 week	1347	1.66188
After 5 week	1248	1.54782
After 7 week	1135	1.41764

4. Conclusions

Nano CP has been successfully synthesized using coprecipitation technique. The optimum condition to attain HAp phase is that the molarities ratio is as 1.5: 0.5 for $CaCl_2$: Na_2HPO_4 respectively. Besides the pH is 7.9 and the reaction temperature is 100 ^oC. Such conditions assisted to have nano CP in HAp phase with crystallite size in order of 6 nm. Having bone - like material with physical properties similar to the natural bone might enhance healing, bioactivity, compatibility and dwindle the possibility of rejection. Nano HAp can be tailored with characteristics resemble the natural human bone species. Gamma-Ray exposure and CT is an active tool for BMD estimation. Such synthesized material can also be used as a simulator for human bone.

REFERENCES

[1] M. Tung, F. Eichmiller, H. Gibson, A. Ly, D. Skrtic, and G. Schumacher, Dentin Desensitization by in situ Formation of Calcium Phosphate, J. Dent. Res. 76 (1997) 2985.

[2] D. M.Liu, Q.Yang, T. Troezynski and W.J.Tsengo, Structural evolution of sol-gel-derived hydroxyapatite. Biomaterials. 23 (2002) 1679-1687.

[3] K. Salma, L.B. Cimdina and N. Borodajenko, Calcium phosphate bioceramics prepared from wet chemically precipitated powders, processing and Application of ceramics 4 (2010) 45-51

[4] L. Sun, C. C. Berndt, A. Kucuk, and K. A. Gross, Material fundamentals and clinical performance of plasma sprayed hydroxyapatite coatings—Review, Appl. Biomat. 58 (2001) 570-592.

[5] R. Z. LeGeros, Calcium Phosphates in Oral Biology and Medicine, Karger, Basel (1991), H. M. Myers, ed., pp. 110-118.

[6] Scott G, King JB. A prospective, double-blind trial of electrical capacitive coupling in the treatment of non-union of long bones. J Bone Joint Surg Am. 76 (1994) 820-826.

[7] R. Kato, S. Nakamura, K. Katayama, and K. Yamashita, Electrical polarization of plasma-spray-hydroxyapatite coatings for improvement of osteoconduction of implants, J. Biomed. Mater. Res 74A (2005) 652

[8] R. Xin, F. Ren, Y. Leng, Synthesis and characterization of nano-crystalline calcium phosphate with EDTA-assisted hydrothermal method, Material and design 31(2010) 1691

[9] Y. Wang, L. Liu, S, Guo, Polymer Degradation Stability, Characterization of biodegradable and cytocompatiblenano-hydroxyapatite /polycaprolactone porous scaffolds in degradation in vitro 95(2010) 207-213

[10] B. D. Kassel, Ph. D. Thesis, University of Berlin (2010)

[11] B.D.Cullity, Elements of X-ray Diffraction, Reading, MA (1959).

[12] www.geol.uni-erlangen.de

[13] www.xpowder.com

[14] K.Salma-Ancane, L.Bērziņa-Cimdiņa, N.Borodajenko. Calcium Phosphate Bioceramics Prepared from Wet Chemically Precipitated Powders. Processing and Application of Ceramics, 4 (2010) 45-51.

[15] S. Jalota, S.B. Bhaduri, A.,, In vitro testing of calcium phosphate (HA, TCP, and biphasic HA-TCP) whiskers", J. Wiley InterScience.,1 (2006) 481–490.

[16] E. Marzec, A comparison of dielectric relaxation of bone and keratin, Bioelectrochemistry and Bioenergetics 46 (1998) 29–32.

[17] K.C.Kao, Dielectric phenomena in solids, Elsevier 2004.

[18] F. Chen, Z.C. Wang, C.L. Lin, Materials Letters, 57 (2002) 858.

[19] Jong HoonKima,b and Sung HoonJeong, Characterization of nano-scaled calcium phosphate particles, J. Ceramic Processing Research. 13 (2012) 32-34.

[20] Brooks R.A., Di Chiro G. Principles of computer assisted

tomography (CAT) in radiographic and radioisotropic imaging. Phys Med Biol. 21(1976) 689–732.

[21] Jing Zhang, Chye Hwang Yan, Chee-Kong Chui, SimHengOng, Accurate Measurement of Bone Mineral Density Using Clinical CT Imaging With Single Energy Beam Spectral Intensity Correction, IEEE Transactions on Image Processing, 29 (2010).

[22] C.E.Orji, Effects of Gamma Irradiation on Some Electrical Properties of Ethylbenzene, Journal of Emerging Trends in Engineering and Applied Sciences 4 (2013) 30-34.